Autosomal-Recessive Hypophosphatemic Rickets Is Associated with an Inactivation Mutation in the *ENPP1* Gene

Varda Levy-Litan,[1,9] Eli Hershkovitz,[2,9] Luba Avizov,[1] Neta Leventhal,[2] Dani Bercovich,[3] Vered Chalifa-Caspi,[4] Esther Manor,[1,5,6] Sophia Buriakovsky,[1] Yair Hadad,[7] James Goding,[8] and Ruti Parvari[1,4,*]

Human disorders of phosphate (Pi) handling and hypophosphatemic rickets have been shown to result from mutations in *PHEX*, *FGF23*, and *DMP1*, presenting as X-linked recessive, autosomal-dominant, and autosomal-recessive patterns, respectively. We present the identification of an inactivating mutation in the ecto-nucleotide pyrophosphatase/phosphodiesterase 1 (*ENPP1*) gene causing autosomal-recessive hypophosphatemic rickets (ARHR) with phosphaturia by positional cloning. ENPP1 generates inorganic pyrophosphate (PPi), an essential physiologic inhibitor of calcification, and previously described inactivating mutations in this gene were shown to cause aberrant ectopic calcification disorders, whereas no aberrant calcifications were present in our patients. Our surprising result suggests a different pathway involved in the generation of ARHR and possible additional functions for ENPP1.

Human disorders of phosphate (Pi) handling and hypophosphatemic rickets have been shown to result from mutations in *PHEX* (MIM 300550),[1] *FGF23* (MIM 605380),[2] and *DMP1* (MIM 600980),[3,4] presenting as X-linked recessive (XLH [MIM 307800]), autosomal-dominant (ADHR [MIM 193100]), and autosomal-recessive patterns (ARHR [MIM 241520]), respectively. These genes have been proposed to act in a common pathway.[5]

The studied pedigree (Figure 1A) was of a family of Bedouin origin. The study was approved by the Soroka Medical University Center institutional review boards, and all patients gave written informed consent before participating.

Patient III1 was referred to the pediatric endocrinology clinic for evaluation of bowing legs at 10 yrs of age. On physical examination, short stature (< 3rd percentile for age), mild dental carries, slight widening of the wrist, and significant valgum deformity of the knee (genu valgum) (Figures S1A and S1B, available online) were noted. He was found to have hypophosphatemia, hyperphosphaturia, elevated plasma alkaline phosphatase, normal levels of serum calcium, normal calcium excretion, PTH and vitamin D metabolites (25OH and 1,25 (OH)2), consistent with hypophosphatemic rickets (Table 1). The patient was treated by phosphates and vitamin D supplements. The response to treatment was inconsistent, and despite wedge osteotomies of the femurs and tibias, the valgum deformity of the knee recurred.

Patient III11 is the cousin of patient III1 and was referred to the pediatric endocrinology clinic for evaluation of short stature at 9 yrs of age. Short stature (<3rd percentile for age), hypoplastic teeth and caries, slight widening of the wrist, and mild genu valgum were noted. X-rays of his left hand revealed delayed bone age and signs of rickets (Figure S1C). Laboratory evaluation confirmed the diagnosis of hypophosphatemic rickets. The abovementioned therapy was offered, but the effect on serum Pi and height was poor. He underwent bilateral wedge osteotomies of the distal femurs, with current successful correction of his deformity.

Patient III4 was examined with the rest of the family members as part of this research project. The patient has normal stature and was apparently healthy except for limping due to delayed healing of a posttraumatic (road accident) fracture of his left distal tibia that occurred 2.5 yrs earlier, requiring several orthopedic operations. Laboratory evaluation disclosed hypophosphatemia and hyperphosphaturia.

Renal function was normal in all patients, and no tubular dysfunction (except for phosphaturia) has been demonstrated. We found no evidence of vascular or periarticular calcifications in X-ray films of the chest, abdomen, and lower limbs of the patients or in abdominal CT of patient III4 (taken after the road accident).

The rest of the family members (parents and siblings) were found to be healthy, without any abnormal clinical or laboratory findings.

Serum FGF23 levels, measured in three experiments with the Elisa Kit of Kainos (Japan) to the full-length biologically active protein, were within the normal range in two

[1]Department of Developmental Genetics and Virology, Faculty of Health Sciences, Ben Gurion University of the Negev, Beer Sheva 84105, Israel; [2]Pediatric Endocrinology & Metabolim Unit, Soroka Medical Center, Beer Sheva 84101 and Faculty of Health Sciences, Ben Gurion University of the Negev, Beer Sheva 84105, Israel; [3]Migal- Galilee Technology Center & Tel Hai Academic College, Kiryat-Shmona 11016, Israel; [4]National Institute of Biotechnology in the Negev, Ben Gurion University of the Negev, Beer Sheva 84105, Israel; [5]Institute of Genetics, Soroka Medical Center, Beer Sheva 84105, Israel; [6]Faculty of Health Sciences, Ben Gurion University of the Negev, Beer Sheva 84105, Israel; [7]Faculty of Agricultural, Food and Environmental Quality Sciences, Hebrew University, Rehovot 76100, Israel; [8]Department of Physiology, Monash University, Victoria 3800, Australia
[9]These authors contributed equally to this work
*Correspondence: ruthi@bgu.ac.il
DOI 10.1016/j.ajhg.2010.01.010.

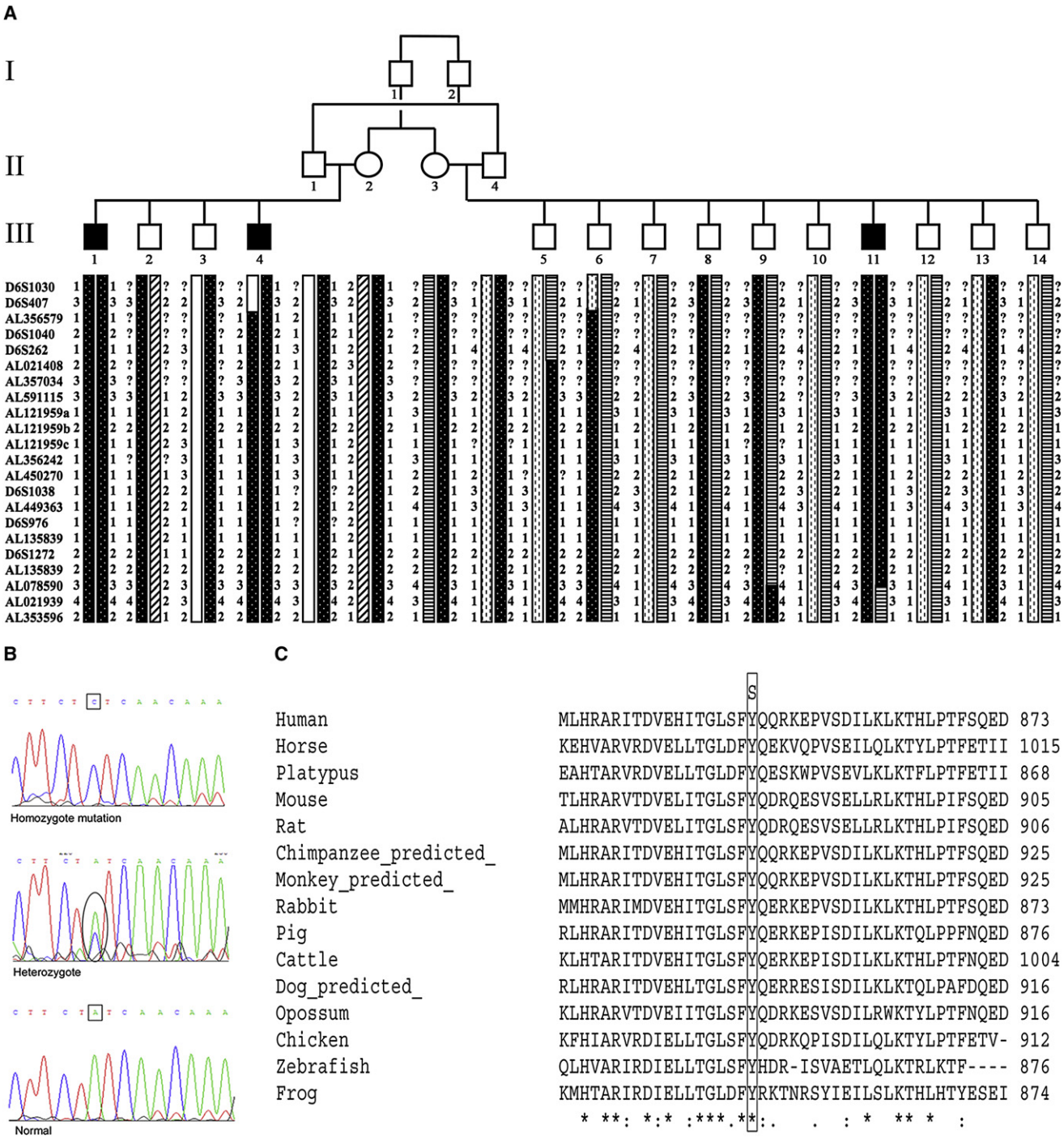

Figure 1. Identification of the Y901S Mutation at the Evolutionarily Conserved Y901 Amino Acid
(A) Haplotype analysis based on microsatellite markers from 6q revealed a founder haplotype (black bar) for which the patient is homozygous in the critical region harboring the *ENPP1* gene. The numbers of the patients correspond to those present in Table 1.
(B) Sequence of the corresponding c.A2722C mutation resulting in Y901S. Patients were homozygous for the mutation, parents and siblings carrying the founder haplotype were heterozygous, and the healthy siblings without the founder haplotype were normal.
(C) Evolutionary conservation of the replaced amino acid Y901. Multiple sequence alignment was carried out by ClustalW. S represents the mutation. Asterisk (*), identical; colon (:), strictly conserved.

patients and were somewhat higher in one patient. This resembles the findings in both XLH patients and patients with mutations in DMP1, in which not all patients showed elevated FGF23 levels.[3,4,6]

After linkage to *PHEX*, *FGF23*, and *DMP1* was excluded, we searched for homozygous regions consistent with linkage by genotyping the three patients and a parent with the Affymetrix (CA, USA) GeneChip Human

Table 1. Clinical and Biochemical Data of ARHR Patients

	Patient III1	Patient III11	Patient III4	Ref. Range
Age (yrs)	19	16	30	
Height (cm)	152	143	165	
Ca (mmol/l)	2.4	2.32	2.45	2.1–2.6
Pi (mmol/l)	0.77	0.68	0.65	0.95–1.75
AP (U/l) (ref. range)	589 (130–350)	480 (150–480)	95 (65–200)	
PTH (pg/ml)	38	18	59	10–65
25OHD (ng/ml)	29	23	34	20–45
$1,25(OH)_2D$ (pg/ml)	27	31	24	19–50
FGF 23 (pg/ml)	50	78	47	10–50
U Ca/Cr (mg/mg)	0.01	0.06	0.05	<0.2
TRP %	80	83	95	85–95
Tp/GFR (ref. range)	2.32 (4.2 ± 0.6)	2.4 (4.2 ± 0.6)	1.7 (3.2 ± 0.5)	

All ions and hormones were measured in serum. Ref. range, reference range. Ca, calcium; Pi, phosphate; AP, alkaline phosphatase; PTH, parathyroid hormone; 25OHD, 25 Hydroxy vitamin D; $1,25(OH)_2D$, 1,25 dihydroxy vitamin D; FGF 23, fibroblast growth factor 23. All were measured in serum after 12 hr fasting, isolated within 30 min after blood withdrawal by centrifugation, and stored at −80°C before biochemical analysis. Because FGF23 is cleaved between Arg^{179} and Ser^{180} and this processing abolishes the biological activity of FGF23,[6] full-length FGF23 levels were measured with a commercial ELISA Kit (Kainos) containing monoclonal antibodies to both the C and N terminus and requiring the presence of both ends for the measurement.[4] U Ca/Cr, urinary calcium to creatinine ratio; TRP %, tubular reabsorption of phosphorus; Tp/GFR, tubular phosphorus reabsorption to glomerular filtration rate ratio.

Mapping 250K Nsp arrays. The genotype calls were determined with Affymetrix Genotyping Console software. Dedicated software (KinSNP) was developed in-house to automatically search the microarray results for homozygous regions consistent with linkage. Three large homozygous regions (>2 cM) were identified, and two were excluded after testing of all family members for microsatellite markers in the regions. Polymorphic markers for the region were developed with the Tandem Repeats Finder,[7] and PCR primers were designed with the use of the Primer3 website. We identified linkage to the chromosomal locus 6q23: 128,856,370–136,244,929 (NCBI Build 36.1) (Figure 1A) with a significant LOD score of 3.45 for D6S262, calculated with Superlink v1.4 at the PedTool server. The calculation was done with the assumption of recessive inheritance with 99% penetrance and an incidence of 0.01 or 0.001 for the disease allele in the population. The multipoint analysis resulted in a LOD score of 4.27.

The linkage interval of 7.39 Mb contains 70 genes, including the *ENPP1* gene, a known player in Pi metabolism.[8] Total RNA was derived from lymphoblastoid cells by the EZ-RNA Reagent (Biologic Industries, Israel). Reverse transcriptase reaction was performed with the Reverse iT 1st Strand Synthesis Kit (ABgene). The cDNA coding region for ENPP1 was directly sequenced on an ABI PRISM 3100 DNA Analyzer with the BigDye Terminator v. 1.1 Cycle Sequencing Kit according to the manufacturer's protocol (Applied Biosystems, CA, USA). The primers that revealed the mutation in the *ENPP1* cDNA were as follows: forward primer, 5′-CCTCTCCCCACCACAACTAA-3′; reverse primer, 5′-TCATGGTGTTTGGGGATAAAA-3′. We identified a nonsynonymous variation (NM_006208.2: c.A2722C, NP_006199.2: p.Y901S) that presented homozygously in all patients and segregated as expected in the healthy family members (Figure 1B). To exclude the possibility that this variation represents polymorphism, we tested 236 Bedouin control individuals of the same geographic region. The primers designed for DNA analysis for screening of the mutation by denaturing high-performance liquid chromatography (DHPLC) amplification of a 192 bp PCR product were as follows: forward primer, 5′-TCCTATTCTCCTAG CATGGGAAGC-3′; reverse primer, 5′-AAACATATCAGTC TTCTTGGC-3′. PCR was performed with high-fidelity Taq polymerase (Fast-Start Taq, Roche). Mutation analysis was performed with the WAVE apparatus from Transgenomic (NE, USA). PCR products were subjected to DNA chromatography.[9] For identification of the homozygous mutation, 10 μl PCR product of wild-type (WT) DNA and 10 μl PCR product of sample DNA were mixed in a 1:1 ratio and denatured at 95°C. This enabled detection of the homozygous mutation by formation of a heteroduplex.

We sought evidence for pathogenic relevance of this variation in multiple sequence alignments of the NPP family of proteins and evolutionary conservation. The tyrosine in position 901 resides in the nuclease-like domain and is strictly conserved in *ENPP1* (Figure 1C), but it is replaced by phenylalanine in *ENPP2* while retaining the three-dimensional structure (not shown). To the best of our knowledge, the three-dimensional structure of the nuclease-like domain is not yet solved; thus, the effect of the amino acid replacement on the protein conformation could not be modeled.

To determine the functional impact of the identified variation in *ENPP1*, we used a previously described full-length

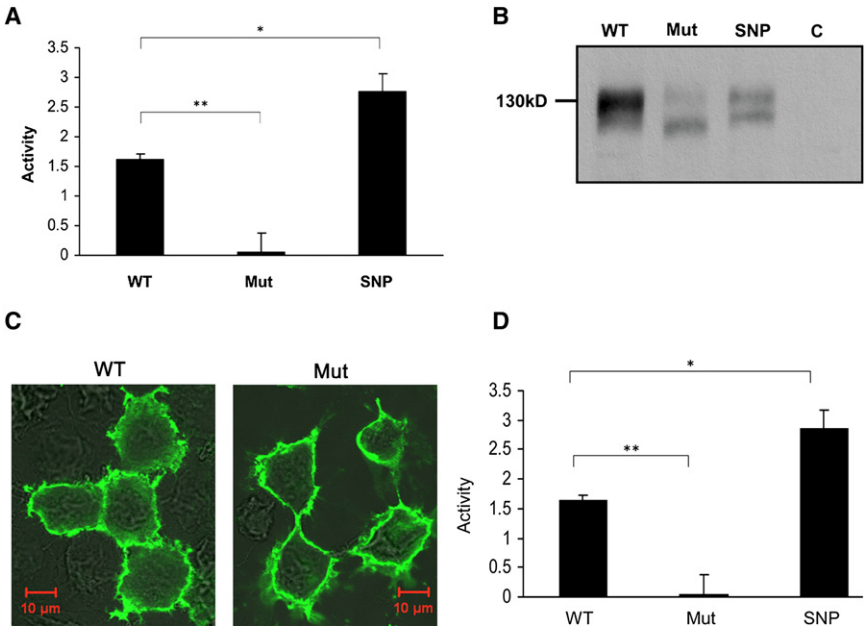

Figure 2. The Effect of the Y901S Mutation and the 779P SNP

(A) ENPP1 activity in intact COS7 cells transfected with the full-length WT human *ENPP1* cDNA (WT), the c.A2722C (Y901S) mutated cDNA (Mut), and the 779P variation (SNP) in pSVT7 expression vectors. Values are expressed as the ratio of NPP activity to time, normalized by total protein concentration and ENPP1 protein levels to correct for transfection efficiency. Untransfected COS7 cells treated in the same way as others served as negative controls, and their background activity was subtracted from the WT, Mut, and SNP activities. ENPP1 levels were determined by immunoblotting and normalized to β-actin. Values are means ± SEM of five independent experiments, each consisting of triplicates of all samples (n = 15). WT: 1.633 ± 0.083. Mut: 0.065 ± 0.302. SNP: 2.775 ± 0.282. *p = 0.006. **p = 0.0002 (two-tailed Student's t test, α level was 0.05; data were tested for normality by the Shapiro-Wilk test).

(B) Representative immunoblot of the ENPP1 protein of WT, Mut, SNP, and negative control. All visible bands resulting from the transfection were used for the normalization to ENPP1 protein levels.

(C) Immunofluorescence staining of COS7 cells transfected with WT and Mut constructs, showing similar membrane localization. Staining performed with the 3E8 mouse monoclonal antibody[13] and secondary antibody Alexa 488 goat anti-mouse IgG. Representative figures of four independent experiments, taken with the Zeiss LSM Axiovert 100 laser scanning microscope. WT scaling (resolution): X, 0.29 μm; Y, 0.29 μm; Z, 0.37 μm. Mut scaling (resolution): X, 0.29 μm; Y, 0.29 μm; Z, 0.32 μm.

(D) ENPP1 activity in lysed COS7 cells transfected with WT, Mut, and SNP constructs. Cells were mechanically lysed by passing through a 21G syringe needle until no pellet was visible. Activity is calculated and represented as in (A). Values are means ± SEM of five independent experiments, each consisting of triplicates of all samples (n = 15). WT: 1.653 ± 0.073. Mut: 0.059 ± 0.328. SNP: 2.869 ± 0.307. *p = 0.0067. **p = 0.0004 (Student's t test).

WT human *ENPP1* cDNA construct in the pSVT7 expression vector[10] to create the c.A2722C mutation, using the QuickChange site-directed mutagenesis protocol with Bioexact Taq polymerase Biolab (LaJolla, CA). The primers used for creating the mutant sequence were as follows: mut forward primer, 5′-CAGCTTCT**C**TCAACAAAGAAAA GAG-3′; mut reverse primer, 5′-CTTTGTTGA**G**AGAAGCT GAGTCC-3′. COS 7 cells were transfected with the mutated and control vectors with TransIT-LT1 Transfection Reagent (Mirus, USA), according to the manufacturer's instructions. Cells treated in the same way as others but without the addition of DNA served as negative controls. Next, 48 hr after transfection, cells were harvested with PBS, and equal portions of about a million cells were separated for measurement of the ENPP1 activity in intact cells, with the use of the membrane-impermeant charged substrate p-nitrophenyl phenyl phosphonate.[11] The remainder of cells were used for immunoblot analyses in order to normalize ENPP1 activity according to transfection efficiency. Protein samples were loaded in graded concentrations, assuring linearity. ENPP1 was detected with the primary rabbit antibody R1702 against the N-terminal cytoplasmic tail,[10] followed by HRP-conjugated anti-IgG anti-rabbit secondary antibody (Jackson ImmunoResearch, PA, USA). To normalize for protein loading, the lower part of the blot was cut and incubated with mouse anti β- actin (Sigma, USA), followed by incubation with HRP- conjugated donkey anti-mouse IgG secondary antibody (Jackson ImmunoResearch). The bound antibodies were visualized with the EZ-ECL Kit (Biological Industries, Israel) and subsequent exposure to X-ray film. Densitometry was measured with the TINA software (Raytest, Straubenhardt, Germany). The ratio of ENPP1 to actin was used to standardize the quantification of enzyme activity. The mutation abolished NPP activity at the cell surface (Figure 2A). We noted that the mutated ENPP1 protein migrates faster than the normal protein (Figure 2B). ENPP1 is a glycosylated ecto-enzyme, with its amino terminus in the cytoplasm and extracellular catalytic domains.[12] The possibility that the faster-migrating mutated protein does not reach the plasma membrane was tested by immunofluorescence staining of intact transfected cells with the 3E8 mouse monoclonal antibody to the native form of ENPP1,[13] followed by Alexa 488-conjugated goat anti-mouse IgG (Molecular Probes). This staining showed that the cell-membrane localization of the mutated protein is comparable to the WT enzyme (Figure 2C). Furthermore, when transfected cells were mechanically lysed by passing through a 21G needle until no pellet was visible, the lysates showed similar relative activities in mutant and WT sequences and enzyme activity was similar to that seen in intact cells, suggesting that in both cases the

majority of the enzyme was located at the cell surface (Figure 2D).

Genetic analysis of rare disorders has identified genes involved in common diseases.[14] The *ENPP1* gene resides in a chromosomal locus that is a suggestive quantitative trait locus for bone loss in rats.[15] Thus, we hypothesized that ENPP1 activity may have a role in this trait; Different polymorphisms in this gene in the human population may alter its enzymatic activity, which in turn will affect bone loss, as observed in the hypophosphatemic patients. We tested a known human SNP for its possible effect on the enzymatic activity (rs1805138; NM_006208.2: c.A2335C; NP_006199.2: p.Thr779Pro). The replacement of the threonine by proline at position 779 in the nuclease-like domain would be expected to result in a major change in the three-dimensional conformation of the enzyme. Indeed, the functional importance of the structure of this domain is demonstrated by the significant reduction of enzymatic activity caused by adjacent mutations C726R, N792S, and R774C.[16] Site-directed mutagenesis was used to create the c.A2335C replacement as above; the primers used were as follows: T727P forward primer, 5′-GAC**C**CCC TACTGCGAAAGTATG-3′; T727P reverse primer, 5′-CAGT AGGG**G**GTCATGAAAGTAGC-3′. The T779P change introduced into the pSVT7 expression vector harboring the full-length *ENPP1* resulted in a significant increase in the enzymatic activity (Figure 2A) and production of a larger proportion of the faster-migrating protein (Figure 2B).

ENPP1 has been shown to have an important role in the generation and disposition of inorganic pyrophosphate (PPi).[8,17] Inactivating mutations in *ENPP1* have previously been reported to cause generalized arterial calcification of infancy (GACI),[16] and inactivation of ENPP1 in mice results in ectopic calcification of joints and ligaments.[18,19] The mutation in our hypophosphatemic patients reduces the activity to about 4% of that of the normal enzyme, similar to the range of activities measured for the mutations causing GACI[16] and resides in the same nuclease-like domain. Specifically, the adjacent mutation K905fsX920 was identified in a severe compound-heterozygous GACI patient who died at 45 days of age[16]. However, we speculate that our patients do not show GACI because of the hypophosphatemia. Alternatively, some in vivo "leakiness" enabling the production of some PPi may save these patients from the calcifications observed in GACI. *ENPP1* has also been demonstrated to have a role in additional aberrant calcification conditions, such as chondrocalcinosis caused by deposition of calcium PPi dehydrate crystals.[20]

Previous studies on human mutants of ENPP1 have found a variable and incomplete reciprocal association between aberrant calcification and hypophosphatemic rickets[16,21]. Because hypophosphataemia can compensate for GACI, it has been argued that this reflects a physiological compensation mechanism rather than a primary defect.[16,21] But unlike previous mutations, the Y901S mutation in our patients results in a phenotype with *complete* dissociation between GACI and ARHR, making a compensatory mechanism an unlikely explanation in this case. At present, we have no explanation, but our results suggest a previously unreported mechanism in the generation of ARHR, maybe via the common FGF23 pathway. A direct effect of ENPP1 on Pi reabsorption may seem unlikely, given that ENPP1 was demonstrated to reside in the distal convoluted tubule of the murine kidney,[22] whereas most Pi reabsorption occurs in the proximal tubule. The closely related ENPP2 is known to have an important additional activity as lysophospholipase D, which explains its biological effects on chemotaxis and angiogenesis.[23,24] The sequences immediately surrounding the active site of ENPP1 and ENPP2 are very similar, and the difference in specificity may reside elsewhere. The separation of GACI and ARHR in different mutations that have in common the loss of ENPP1 activity may suggest that, like ENPP2, ENPP1 may have more than one important biological activity.

Supplemental Data

Supplemental Data include one figure and can be found online at http://www.ajhg.org.

Acknowledgments

We wish to thank the family members for their collaboration. We thank El-Ad David Amir and Ofer Bartal for their contribution to the development of KinSNP. This study was funded in part by a grant from the Israeli Ministry of Health to R.P and E.H.

Received: October 23, 2009
Revised: December 23, 2009
Accepted: January 11, 2010
Published online: February 4, 2010

Web Resources

The URLs for data presented herein are as follows:

ClustalW, http://www.ebi.ac.uk/Tools/clustalw2/index.html
KinSNP, http://bioinfo.bgu.ac.il/bsu/software/KinSNP/
Online Mendelian Inheritance in Man (OMIM), http://www.ncbi.nlm.nih.gov/Omim/
PedTool, http://bioinfo.cs.technion.ac.il/superlink/
Primer3, http://frodo.wi.mit.edu/cgi-bin/primer3/primer3_www.cgi

References

1. The HYP Consortium. (1995). A gene (PEX) with homologies to endopeptidases is mutated in patients with X-linked hypophosphatemic rickets. Nat. Genet. *11*, 130–136.
2. ADHR Consortium. (2000). Autosomal dominant hypophosphataemic rickets is associated with mutations in FGF23. Nat. Genet. *26*, 345–348.
3. Feng, J.Q., Ward, L.M., Liu, S., Lu, Y., Xie, Y., Yuan, B., Yu, X., Rauch, F., Davis, S.I., Zhang, S., et al. (2006). Loss of DMP1 causes rickets and osteomalacia and identifies a role for osteocytes in mineral metabolism. Nat. Genet. *38*, 1310–1315.

4. Lorenz-Depiereux, B., Bastepe, M., Benet-Pagès, A., Amyere, M., Wagenstaller, J., Müller-Barth, U., Badenhoop, K., Kaiser, S.M., Rittmaster, R.S., Shlossberg, A.H., et al. (2006). DMP1 mutations in autosomal recessive hypophosphatemia implicate a bone matrix protein in the regulation of phosphate homeostasis. Nat. Genet. *38*, 1248–1250.
5. Schiavi, S.C. (2006). Bone talk. Nat. Genet. *38*, 1230–1231.
6. Yamazaki, Y., Okazaki, R., Shibata, M., Hasegawa, Y., Satoh, K., Tajima, T., Takeuchi, Y., Fujita, T., Nakahara, K., Yamashita, T., and Fukumoto, S. (2002). Increased circulatory level of biologically active full-length FGF-23 in patients with hypophosphatemic rickets/osteomalacia. J. Clin. Endocrinol. Metab. *87*, 4957–4960.
7. Benson, G. (1999). Tandem repeats finder: a program to analyze DNA sequences. Nucleic Acids Res. *27*, 573–580.
8. Terkeltaub, R. (2006). Physiologic and pathologic functions of the NPP nucleotide pyrophosphatase/phosphodiesterase family focusing on NPP1 in calcification. Purinergic Signal. *2*, 371–377.
9. Bercovich, D., and Beaudet, A.L. (2003). Denaturing high-performance liquid chromatography for the detection of mutations and polymorphisms in UBE3A. Genet. Test. *7*, 189–194.
10. Belli, S.I., and Goding, J.W. (1994). Biochemical characterization of human PC-1, an enzyme possessing alkaline phosphodiesterase I and nucleotide pyrophosphatase activities. Eur. J. Biochem. *226*, 433–443.
11. Kelly, S.J., and Butler, L.G. (1975). Enzymic hydrolysis of phosphonate esters. Biochem. Biophys. Res. Commun. *66*, 316–321.
12. Goding, J.W., Grobben, B., and Slegers, H. (2003). Physiological and pathophysiological functions of the ecto-nucleotide pyrophosphatase/phosphodiesterase family. Biochim. Biophys. Acta *1638*, 1–19.
13. Solan, J.L., Deftos, L.J., Goding, J.W., and Terkeltaub, R.A. (1996). Expression of the nucleoside triphosphate pyrophosphohydrolase PC-1 is induced by basic fibroblast growth factor (bFGF) and modulated by activation of the protein kinase A and C pathways in osteoblast-like osteosarcoma cells. J. Bone. Min Res. *11*, 183–192.
14. Peltonen, L., Perola, M., Naukkarinen, J., and Palotie, A. (2006). Lessons from studying monogenic disease for common disease. Hum. Mol. Genet. *15*(Spec No 1), R67–R74.
15. Koller, D.L., Liu, L., Alam, I., Sun, Q., Econs, M.J., Foroud, T., and Turner, C.H. (2008). Epistatic effects contribute to variation in BMD in Fischer 344 x Lewis F2 rats. J. Bone Miner. Res. *23*, 41–47.
16. Rutsch, F., Ruf, N., Vaingankar, S., Toliat, M.R., Suk, A., Höhne, W., Schauer, G., Lehmann, M., Roscioli, T., Schnabel, D., et al. (2003). Mutations in ENPP1 are associated with 'idiopathic' infantile arterial calcification. Nat. Genet. *34*, 379–381.
17. Terkeltaub, R.A. (2001). Inorganic pyrophosphate generation and disposition in pathophysiology. Am. J. Physiol. Cell Physiol. *281*, C1–C11.
18. Okawa, A., Ikegawa, S., Nakamura, I., Goto, S., Moriya, H., and Nakamura, Y. (1998). Mapping of a gene responsible for twy (tip-toe walking Yoshimura), a mouse model of ossification of the posterior longitudinal ligament of the spine (OPLL). Mamm. Genome *9*, 155–156.
19. Sali, A., Favaloro, J.M., Terkeltaub, R., and Goding, J.W. (1999). Germline deletion of the nucleoside triphosphate pyrophosphohydrolase (NTPPPH) plasma cell membrane glycoprotein (PC-1) produces abnormal calcification of periarticular tissues. In Ecto-ATPases and Related Ectonucleotidases, L. Vanduffel and R. Lemmens, eds. (Maastricht, The Netherlands: Shaker Publishing BV), pp. 267–282.
20. Rutsch, F., and Terkeltaub, R. (2005). Deficiencies of physiologic calcification inhibitors and low-grade inflammation in arterial calcification: lessons for cartilage calcification. Joint Bone Spine *72*, 110–118.
21. Ciana, G., Trappan, A., Bembi, B., Benettoni, A., Maso, G., Zennaro, F., Ruf, N., Schnabel, D., and Rutsch, F. (2006). Generalized arterial calcification of infancy: two siblings with prolonged survival. Eur. J. Pediatr. *165*, 258–263.
22. Harahap, A.R., and Goding, J.W. (1988). Distribution of the murine plasma cell antigen PC-1 in non-lymphoid tissues. J. Immunol. *141*, 2317–2320.
23. Tokumura, A., Majima, E., Kariya, Y., Tominaga, K., Kogure, K., Yasuda, K., and Fukuzawa, K. (2002). Identification of human plasma lysophospholipase D, a lysophosphatidic acid-producing enzyme, as autotaxin, a multifunctional phosphodiesterase. J. Biol. Chem. *277*, 39436–39442.
24. Umezu-Goto, M., Kishi, Y., Taira, A., Hama, K., Dohmae, N., Takio, K., Yamori, T., Mills, G.B., Inoue, K., Aoki, J., and Arai, H. (2002). Autotaxin has lysophospholipase D activity leading to tumor cell growth and motility by lysophosphatidic acid production. J. Cell Biol. *158*, 227–233.